



## DESIGN, TESTING AND IMPLEMENTATION OF TADAS DEVICES IN THREE RC BUILDINGS WITH SHEAR WALLS AND COUPLING BEAMS

R. Zemp<sup>(1)</sup>, R.C. Urrutia<sup>(2)</sup>, M. Rendel<sup>(3)</sup>, G. Cavalla<sup>(4)</sup>, J.C. de la Llera<sup>(5)</sup>

<sup>(1)</sup> Technical Manager, Nüyün\_Tek S.p.A., [rzemp@nuyuntek.cl](mailto:rzemp@nuyuntek.cl)

<sup>(2)</sup> Project Manager, Nüyün\_Tek S.p.A., [rurrutia@nuyuntek.cl](mailto:rurrutia@nuyuntek.cl)

<sup>(3)</sup> Technical Manager, SIRVE Seismic Protection Technologies S.A., [mrendel@sirve.cl](mailto:mrendel@sirve.cl)

<sup>(4)</sup> General Manager, CRL Ingeniería Estructural S.p.A.

<sup>(5)</sup> Principal Investigator, National Research Center for Integrated Natural Disaster Management (CIGIDEN), CONICYT/FONDAP/15110017, School of Engineering, Pontificia Universidad Católica de Chile, [jllera@ing.puc.cl](mailto:jllera@ing.puc.cl)

### Abstract

A Triangular Added Damping and Stiffness (TADAS) device is an economic energy dissipation solution to improve the earthquake performance of flexible buildings. TADAS devices have a very stable force displacement constitutive relationship and a high capability of energy dissipation. This research proposes the use of TADAS dampers in coupling beams or lintels between reinforced concrete (RC) shear walls. Coupling beams are typical of RC shear wall buildings with flat slabs and staircase and elevator shear wall cores. The proposed solution integrates into the structure without a relevant impact on the architecture, a significant advantage over other energy dissipation solutions. In this article, three different building applications with TADAS devices are presented. Numerical simulations for these buildings show that drift, displacement, and base shear reductions typically range between 10% and 30%. An effective TADAS design balances stiffness, energy dissipation, and fatigue life of the device under cyclic plastic deformations. Fatigue life for mild steel was determined experimentally and the TADAS devices were designed with a simple model validated by testing of single triangular plates. As expected for rate independent plasticity, tests at different frequencies showed negligible performance variations with deformation velocity. Several TADAS prototypes were cyclically tested and their results are reported in this article. In an effort to analyze the performance and stiffness of the connection between the damper and RC beam, the prototype tests include a section of the capacity-designed concrete beam with the device under simulated as-built conditions. The final design also allows replacing the damper, if needed, after a strong earthquake, and considers an installation procedure that minimizes slip in the connection to the concrete beam.

*Keywords: Triangular Added Damping and Stiffness (TADAS); Energy Dissipation; RC Building; Building Implementation.*



## 1. Introduction

Nowadays, using energy dissipation devices is a well-accepted solution within the engineering community to improve the seismic performance of new and existing buildings. Metallic damping devices, such as the “Added Damping and Stiffness” (ADAS), “Triangular Added Damping and Stiffness” (TADAS), or Shear Panel are energy dissipation devices which add stiffness and damping to the structure. They present the typical hardening elasto-plastic constitutive behavior that is well known in metallic dampers. These devices are often made of steel [1]-[2], but other metals such as copper and stainless steel have also been developed [3]-[5].

Compared to other energy dissipating devices, for example the more frequently implemented viscous damper, metallic damping devices have the advantage that the theory and manufacturing technology and process is simple and well understood. A disadvantage of metallic dampers relative to viscous dampers is the accumulated plasticity or memory of the metallic material. Depending on the design of the damper, after a severe earthquake metallic dampers may need replacement to endure a future event. In the case of TADAS devices, different aspects of their behavior have been considered in literature, such as the effect of the added stiffness to the structure, period reduction, damping, response modification factor, effect of distance between triangular plates, and the optimization of the height-wise distribution of the dampers [6]-[9].

On the other hand, Reinforced Concrete (RC) walls are commonly used in several countries as the preferred lateral force resisting system for medium and high-rise buildings [10]. Often these walls are coupled by beams to improve the resistance of single acting walls. When designed in a ductile manner, these coupling beams may act as fuses to dissipate the seismic energy [11]. This means that for a strong motion earthquake, major damage has to be accepted in these fuse beams and retrofit of these structural elements is needed after the earthquake, which implies additional costs and disturbance to the building occupants. Therefore, using metallic damping devices in coupling beams is a convenient solution to concentrate the energy dissipation in devices with a large deformation capacity, thus protecting the coupling beams. In references [12]-[16], the performance of such metallic damping devices in RC coupling beams was studied. Some implementation examples of metallic dampers are the use of TADAS devices in the Core Pacific Shopping Center in Taiwan [17]-[18], ADAS devices in the retrofitting of the Wells Fargo Bank Building in San Francisco, California [19], the ADAS retrofit of the Izazaga building, the Cardiology Hospital buildings, and the Reforma buildings in Mexico City [20], and recently the use of a dual function metallic damper in a building on the campus of the Dalian University of Technology in China [21].

Using energy dissipation devices in coupling beams of RC walls is an economically affordable way to add energy dissipation into a structure because no additional metallic elements, such as braces, are needed and the proposed solution has negligible architectural impact. In this article, the design, testing, and implementation of TADAS devices in coupling beams of three RC buildings to improve seismic performance is presented. First, numerical simulation results are presented for the three buildings with TADAS devices. Then, a simple model to design the TADAS devices and to predict the force capacity and fatigue life of the devices is discussed. Two different connection types of the fixed end of the TADAS to the coupling beam are proposed. Also, single plate tests were performed for the design of the devices and special tests were performed to evaluate: (i) dependency of the constitutive force displacement relationship with deformation velocity and (ii) the relationship between maximum deformation and fatigue life. Real scale prototypes for the buildings were manufactured and tested and the results are presented herein. Finally, different aspects of the implementation of the TADAS devices for the three buildings presented are discussed. All buildings were constructed between 2013 and 2015.

## 2. Buildings and simulation results with TADAS devices

This section presents the implementation of TADAS devices in three recently built RC buildings. The primary objective was to reduce deformation in the structure and increase earthquake safety. Several damper alternatives had to be considered since one of the restrictions was to abide by the already completed structural and architectural layout in two of the three projects. It was challenging to find specific locations for the devices to improve the performance of the structure in a significant way without altering the architecture or load paths in the structure. For privacy reasons, the buildings will be denoted with letters A, B, and C.

Building A, a 24-story reinforced concrete building is a textbook case structure, composed of a shear wall core with a perimeter frame. The vertical members are arranged in a 3x3 grid with spans of approximately 8.5 m in length, the center square of the grid roughly corresponds to the shear wall core. The TADAS devices are located in a single direction of the building, so they couple the vertical deformations of two shear walls. Two devices were installed in each story with capacities as follows: (a) 340 kN for the devices installed between the 2nd and 6th stories; (b) 600 kN for the devices installed between the 7th and 10th stories; and (c) 510 kN for the devices installed between the 11th and 21st stories.

Building B is a 30-story reinforced concrete office tower. The structure is composed of a shear wall core and a mixed wall and frame structure in the rest of the plan. In particular, one direction of the building is considerably more resistant than the other since all the walls are oriented in one direction. The tower has plan dimensions of 25 m by 30 m at the base with a height-wise tapering section. The dampers were installed at the building core by coupling short shear walls in the weaker direction. Three devices with a nominal capacity of 360 kN were installed in each story between the 2nd and 21st stories, and two devices per story with 540 kN capacity were installed between the 22nd and 30th stories.

Building C is a 27-story reinforced concrete office tower with a mixed shear wall and frame structure. The structure has a shear wall core and several wall distributed along the perimeter for added stiffness. The tower has plan dimensions of 43 m by 33 m on the first 19 stories, and then reduces to 43 m by 16 m in the upper stories. The dampers were installed to couple the shear walls of the building core. All dampers work in the same direction. Four devices with a nominal capacity of 260 kN were installed in each story between the 1st and 13th stories, and three devices with 520 kN capacity were installed between the 14th and 27th stories.

Figure 1 schematically presents a TADAS device installed between beams coupling two walls in a manner that is representative of the one used in all building implementations presented in this article. One side of the device is fixed to the beam, and the other side has pinned connections. Both sides of the device are connected directly to the rebar of the cantilever beam segments. A capacity design of the coupling beams ensures that they remain elastic during the earthquake.

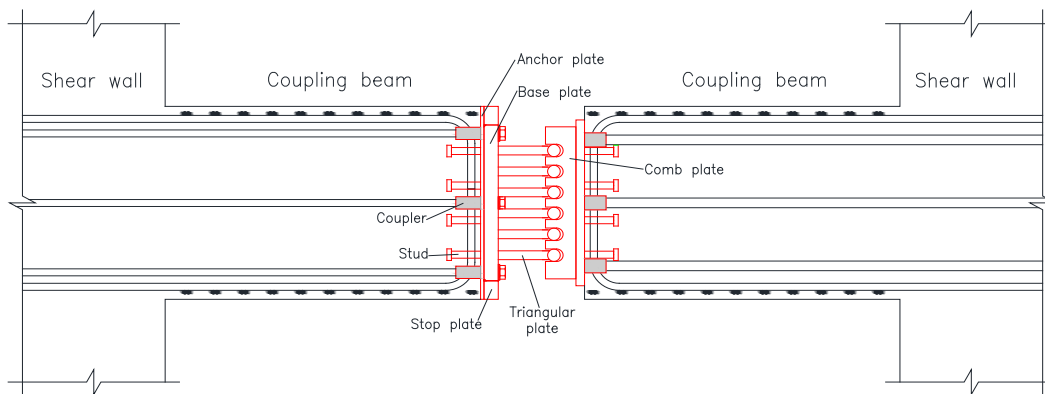


Figure 1 - Schematic representation of the typical connection of TADAS devices in buildings.

The buildings were modeled using the commercial software ETABS version 9.7.4 [22] and use linear-elastic properties to represent the behavior of the structural elements such as walls, columns and beams. The dampers were modeled using non-linear elements with independent uniaxial plasticity properties. The plasticity model is based on the hysteretic behavior proposed by Wen [23], in which all internal deformations are independent, i.e. the yielding of one deformation does not affect the behavior of other deformations in the device. For the particular application of TADAS devices, these shortcomings are not of particular concern since the devices work mainly in a single direction.

Linear analyses in ETABS are based on effective-damping properties and ignore cross coupling modal terms. As such, they grossly misrepresent the amount of damping present in the structure when energy dissipation devices are introduced. Therefore, it is crucial to use nonlinear time-history analysis to study the effects of introducing

these devices on any structure, either to estimate the demand reduction on structural members, or to estimate the local forces and displacements imposed on the TADAS devices and their anchoring elements.

The devices and their anchoring elements were designed using the envelope results from inelastic modal time history analyses considering a 5% modal damping, using three ground motions compatible with the Chilean design spectrum for a maximum possible earthquake (10% probability of being exceeded in 100 years). No response modification factor was used for the design of the TADAS devices. Shown in Figure 2 (a) are the artificial ground motions used for the design of Building A. These ground motions were developed based on seed records from the March 3<sup>rd</sup>, 1985 Viña de Mar earthquake recorded on the same soil type as the one present in the structure. Shown in Figure 2 (b) is the matching of these ground motions to the code spectrum, where it is shown that the match is very good, especially in the region above 1s, where the natural periods of all the considered buildings are located.

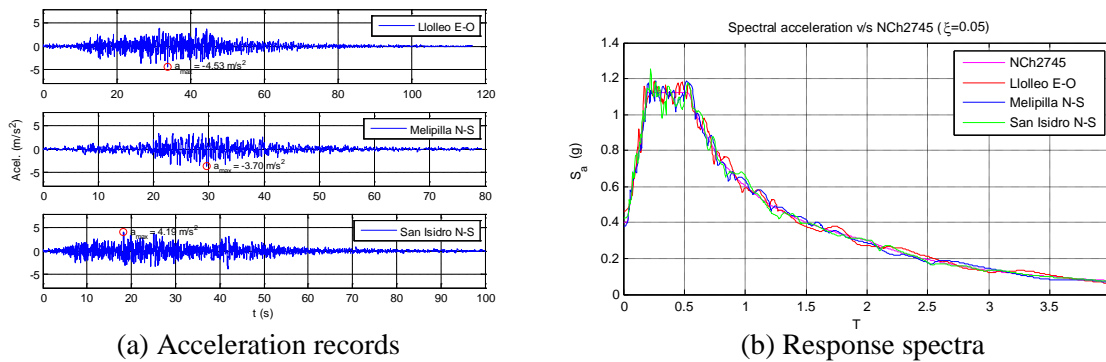


Figure 2 - Spectrum compatible ground motions used in design.

Figure 3 shows a comparison of the maximum inter-story drifts associated with the envelope of the design earthquakes of the NCh2745 code [24] - 10% probability of being exceeded in 50 years - evaluated with and without the TADAS devices. Reductions above 10% are observed in most of the stories, with reductions of at least 20% in the story drift of the first story, and peak reductions above 30% in some cases. It is also worth mentioning that only for a few stories, e.g., the last story of Building C, this reduction is negligible.

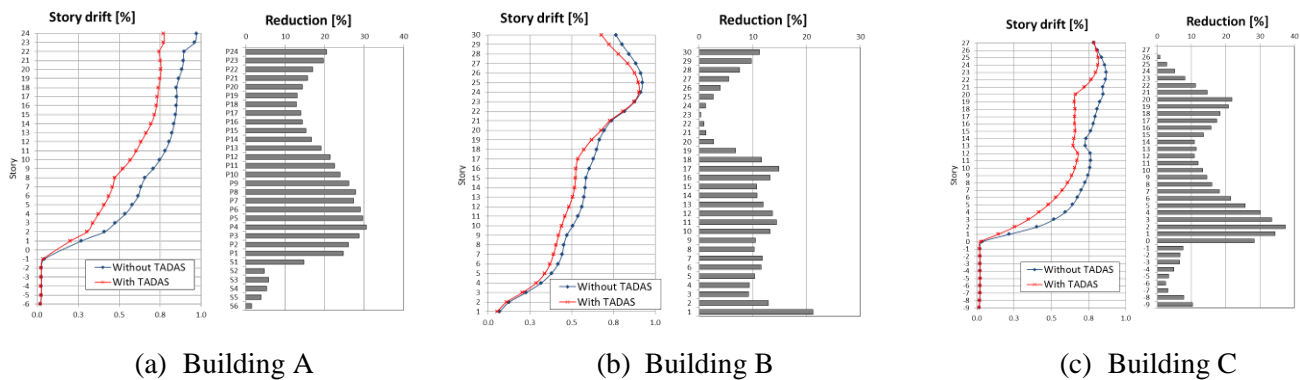


Figure 3 - Story drift reductions.

Table 1 summarizes some key indicators of the improvement in performance introduced into the buildings by the TADAS devices. The results are computed as the average reductions obtained from the three earthquake records used in building design. Considering that the internal modal damping assumed in these structures was 5%, which is high, the results presented probably underestimate the real performance of the TADAS devices. Nevertheless, it can be seen that the primary objective of reducing the deformations, represented in the Table by the root mean square (RMS) of the interstory drifts is achieved, reaching an average reduction of 21.8% and values ranging from 14.6% to 30.6%. It is also important to note that despite not being a primary design objective, important reductions are achieved for the roof displacement and roof acceleration. Although the base shear has rarely an effect on the design of tall structures, a considerable reduction can be observed as well in this response. In



summary, it is apparent that the implementation of TADAS devices is unequivocally beneficial to the structural performance, where reductions are achieved in all performance indicators.

Table 1 - Average reduction of structural performance indicators

	RMS interstory Drift (%)	Total peak Roof Acceleration (%)	Roof Displacement (%)	Base Shear (%)
Building A	20.2	5.0	32.1	16.1
Building B	30.6	16.7	24.6	15.8
Building C	14.6	24.9	12.0	12.2

### 3. TADAS design

Metallic dampers as TADAS, ADAS or Shear Panels dissipate energy by plastic deformation. In the current implementation, relative vertical displacement of the ends of the coupling beams between shear walls produces the plastic deformation in the device during an earthquake. Due to large displacements of the triangular plates in such event, these types of devices develop considerable levels of axial forces in the coupling beam. The levels of axial forces for these three metallic dampers were simulated considering the non-linear elasto-plastic behavior of the material. For the sake of brevity this results cannot be presented herein but it is concluded that the levels of axial forces are considerably lower in the case of TADAS compared to ADAS or Shear panels. Therefore, TADAS devices were selected for the presented real implementation. In the case of TADAS devices, one end is fixed to the coupling beam while the other end is pinned. In the case of ADAS devices or Shear Panels, both ends are fixed to the coupling beams and for large displacements of these two dampers, significant levels of axial forces occurs while, in the case of the TADAS device, the pinned connection generates lower levels of axial force produced by some friction in the pinned connection.

The triangular plates of the TADAS device are made of special mild steel with high ductility. Copper or stainless steel elements would have even better ductility [3]-[5] but mild steel was preferred for its low cost and simplicity of the manufacturing process. To release residual stresses in the triangular plates of the TADAS device, which results from the manufacturing process, say welding, a special heat treatment is applied.

The triangular plates of a TADAS device can be designed with a simple model as proposed in [1] and [2]. The flexural moment distribution over the length of the TADAS device has a triangular shape starting in zero at the pinned end and ending in  $M = F \times L$  at the fixed end of the triangular plate, where  $F$  is the developed force of the triangular plate and  $L$  is the length between pinned and fixed end. Due to the triangular shape of the TADAS plate, it can be assumed that stresses produced by the flexural moment are constant over the length of the triangular plate. So the triangular plate can deform well into inelastic range without a curvature localization. Based on this assumption the curvature of a triangular plate has the shape of a section of a circle and the displacement  $w$  at the pinned end depends on the strain  $\epsilon$ , the thickness  $h$  of the plate, and its length  $L$ :

$$w = \frac{h}{2\epsilon} \cdot \left[ 1 - \cos\left(\frac{2L\epsilon}{h}\right) \right] \quad (1)$$

Equation (2) shows the plastic force  $F$  of the triangular plate that depends on the geometry of the plate, where  $b$  is the width of the triangular plate;  $f_y(\epsilon)$  the stress strain constitutive relationship; and  $f_h$ , a factor to account for the hardening of the material, both defined experimentally.

$$F = \frac{bh^2}{4L} \cdot f_y(\epsilon) \cdot f_h \quad (2)$$

With Equations. (1) and (2), the force relationship  $F-w$  is defined. As the TADAS is a metallic device which dissipates energy by plastic deformation, the strain fatigue life cycle relationship has to be defined for the used material, considering manufacturing conditions as for example welding, which adds residual stresses, and heat treatment, which releases part of these stresses. In Figure 4 a typical relationship obtained by dynamic testing for the used material and manufacturing process is shown. An efficient design of a TADAS device is a trade-off

between a high number of fatigue cycles and a large stiffness of the devices. The smaller the number of fatigue cycles the stiffer the devices. In other words, as  $L$  decreases, the stiffness of the triangular plate increases. For a given displacement  $w$  and considering Equation (1), it can be seen that the strain  $\epsilon$  increases as the length  $L$  decreases. And from Figure 4 it is observed that the higher the strain  $\epsilon$ , the smaller the number of fatigue life cycles.

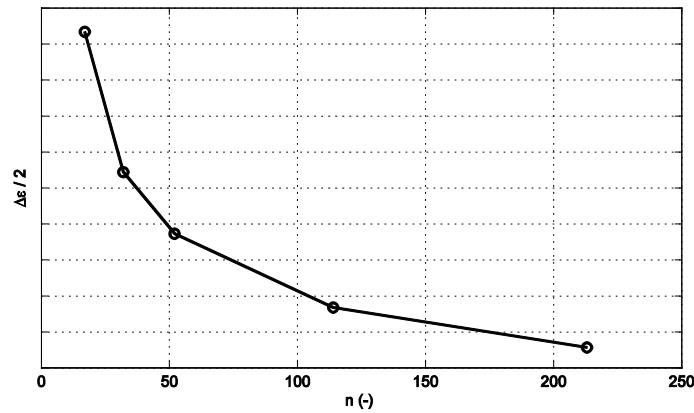


Figure 4 - Strain versus number of fatigue life cycles.

Two different types of the fixed connections of the triangular plates to the coupling beam were implemented in the three different buildings. For Building A, a fixed connection Type I and for Buildings B and C a Type II were implemented. In Figure 5, pictures of the prototype installed in the testing machine with connection Type I (part (a)) and in Figure 5 (part (b)) for connection Type II are presented. In the configuration Type I, three prestressed bolts holds the package of triangular plates together, while for Type II the triangular plates are welded to a base plate. The Type II connection has the advantage that the triangular plates can be assumed as totally fixed, however in configuration Type I, some rotation of the triangular plates must be assumed, which decreases the stiffness of the device. The Type I connection has the advantage that no welding is necessary, so there are no residual stresses added due to welding, and hence an improved fatigue life. Depending on the objective in the design of the energy dissipation system, Type I or Type II connections were selected for different buildings.



(a) Prototype Building A, Type I connection.



(b) Prototype Building B, Type II connection.

Figure 5 - Prototype TADAS devices installed in test machine.

In Table 2 some parameters of the designed TADAS are summarized. The geometry of the triangular plates is different for the three buildings. The design and maximum displacement presented in the Table were obtained from simulation of the building structures described earlier considering the design and maximum earthquake, respectively. The nominal total force capacity for maximum displacement of the TADAS devices is the product



of the number of plates times the nominal force  $F$  presented in the Table and obtained from Equation 2. The energy specified in Table 2 is obtained from simulations for the maximum earthquake. The objective in the design was that the TADAS devices should have the capacity to dissipate at least twice the specified energy. Hence the TADAS devices do not have to be replaced for the expected life of the buildings; however, the bolted connection to the coupling beam permits a replacement, if necessary.

Table 2 - Summary of the designed TADAS devices for the three buildings.

	# of implemented TADAS	Fixed connection type	Design displ. (mm)	Maximum displ. (mm)	# of triangular plate per TADAS	Nominal force $F$ per plate (kN)	Dissipated energy per plate (kJ)
Building A	40	I	62	70	4, 6 & 7	85	214
Building B	78	II	27	31	4 & 6	90	101
Building C	94	II	30	43	3 & 6	88	116

#### 4. Single plate testing

For the three buildings with TADAS devices of different geometries, cyclic tests were performed on single triangular plates to evaluate the design just described. The MTS actuator used at the Dynamic Testing Laboratory at Pontificia Universidad Católica de Chile has a stroke of  $\pm 250$  mm, a nominal force capacity of 250 kN, and reaches peak velocities of about 500 mm/s. The triangular plates were tested with different amplitudes and frequencies. In Figure 6 cyclic sinusoidal tests with maximum amplitude specified in Table 2 are presented. In plots (a) to (c), tests for the TADAS device of Buildings A to C are presented at a frequency of 0.1 Hz, respectively, while in (d) the frequency was 1.2 Hz for the TADAS device of Building B. Testing was finished when fatigue failure occurred, excepted for the test presented in Figure 6 (a), in which testing was stopped before the triangular plate failed. Fatigue failure was defined when the force decreased to 85% of the maximum force measured in the test.

In Figure 6 the predicted force displacement relationship is superimposed with a red line to the tested constitutive force-deformation curve. It can be seen that the prediction of the force displacement with the simple model used in the design is satisfactory. In some cases the difference between measured and predicted results is larger; this difference is attributed to a variation of the properties of the mild steel since for the three projects triangular plates were manufactured from different steel batches.

The force-deformation constitutive relationship of the triangular plates shown in Figures 6 (b) and (d) have the same geometry, were manufactured from the same batch of steel, and were tested at different frequencies. The difference in peak force measured in the first 10 cycles is only 1.6%. After these cycles, slightly larger differences were observed. Also, the number of cycles at which fatigue failure occurred was very similar. As assumed for mild steel, test velocity has a very small influence in the constitutive relationship of the TADAS, so the test can be performed at lower velocities than the ones imposed by the earthquake.

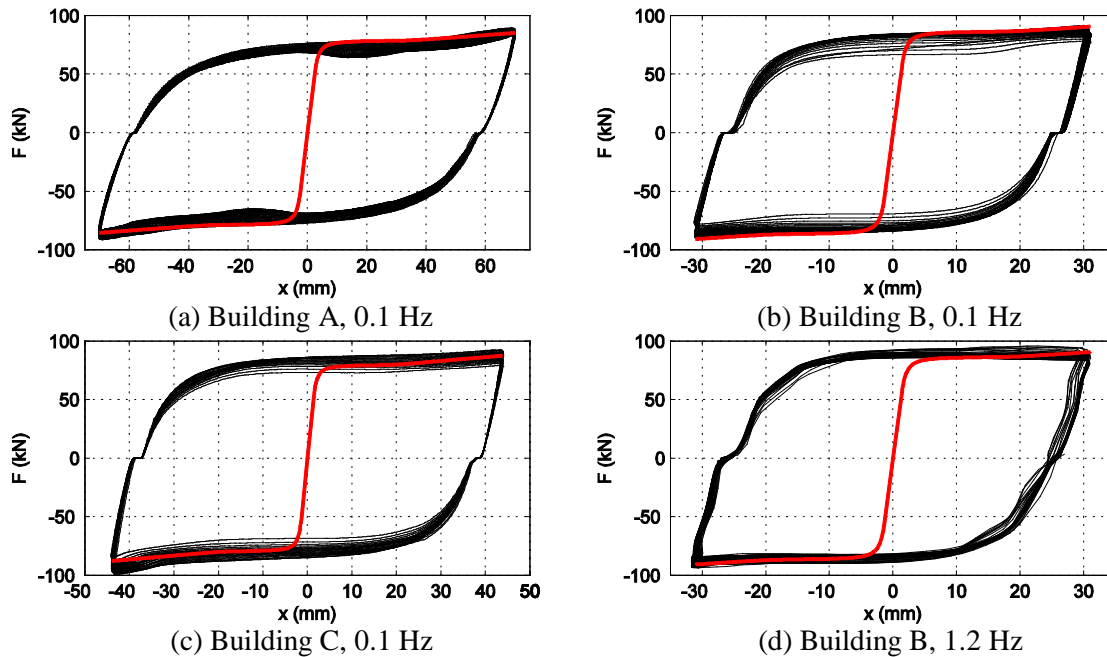


Figure 6 - Force displacement relationship of triangular plates for different buildings, maximum displacement tests and different frequencies.

The energy dissipated by the triangular plates, which test results are presented in Figures 6 (a) to (d) is 700 kJ, 458 kJ, 336 kJ and 421 kJ, respectively. Comparing these values with the specified maximum energy defined in the design and presented in Table 2, it can be seen that the dissipated energy in these tests is between 2.9 and 4.2 times larger than the maximum design energy.

For the geometry of the triangular plates implemented in Project B, different tests with different amplitudes were performed. Figure 7 shows the obtained relationship between amplitude versus dissipated energy. It is observed that the dissipated energy does not depend strongly on the test amplitude of the triangular plate. In a first approximation, it could be safely assumed that the dissipated energy is nearly independent from the amplitude and hence from the strain  $\epsilon$ . This observation legitimates to test the TADAS devices designed for an earthquake implementation at constant amplitude tests.

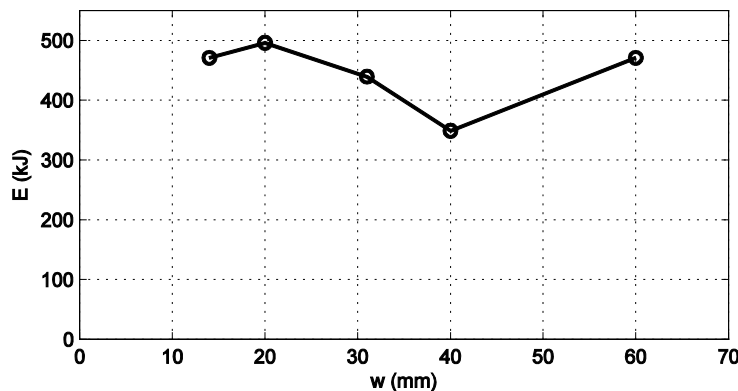


Figure 7 - Displacement versus dissipated energy

## 5. Prototype testing

For each of the three projects presented, two real scale prototypes were manufactured and tested. The tests were performed on the MTS actuator of the PUC Laboratory. The actuator has a nominal maximum capacity of

1000 kN, a maximum stroke of  $\pm 500$  mm, and reaches a peak velocity of about 160 mm/s. The used test set-up is shown in Figure 8. To evaluate the performance of the anchorage system of the TADAS devices, a part of the beam in reinforced concrete was reproduced as shown in this Figure.

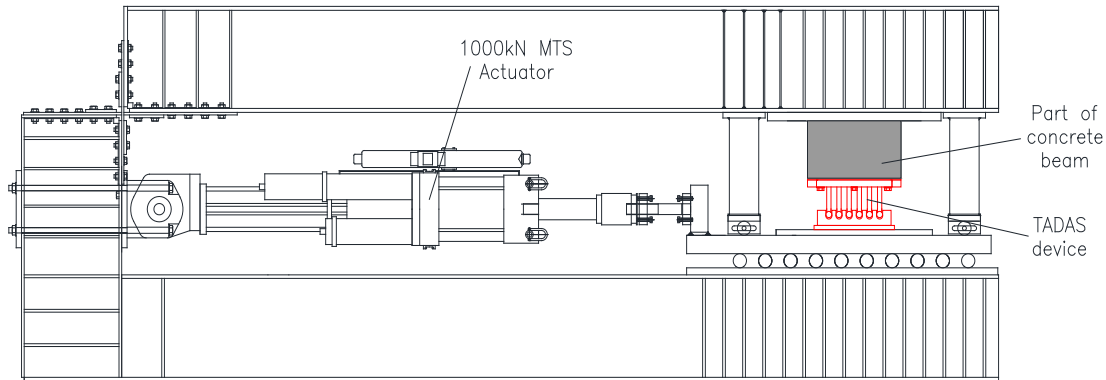


Figure 8 - Experimental set-up of prototype testing.

In Figures 9 (a) to (c) the constitutive force displacement relationship obtained from the prototype tests is presented for Buildings A, B, and C, respectively. The frequency was 0.1 Hz for all these tests. The prototype for Building A was tested for the maximum amplitude (Table 2) and for Building B and C, cycles with design and maximum displacements were performed. In these two cases, not all the cycles of maximum amplitude tests are plotted. By comparing the design with the maximum amplitude tests, hardening of the material was observed. As already observed in single plate tests, the TADAS devices show a stable constitutive behavior. Comparing the results to the single plate tests, it can be stated that no major difference in terms of energy dissipation, force-deformation constitutive behavior, or maximum force capacity was observed. The efficiency  $E_c / ((F_{max} - F_{min}) \times (w_{max} - w_{min}))$  calculated for these tests is 65.6%, 80.4% and 80.2% for the prototypes of Buildings A, B and C, respectively.  $E_c$  is the energy dissipated in the cycle in which maximum force is obtained and  $F_{max}$ ,  $F_{min}$ ,  $w_{max}$  and  $w_{min}$  are the maximum and minimum force, and maximum and minimum displacement of this cycle, respectively. The efficiency of the TADAS device for Building A is smaller than that obtained for Buildings B and C. This is due to two reasons. First, as already mentioned in a previous section, the fixed connection Type II (Buildings B and C) is stiffer than the Type I connection (Building A) and second, in the case of the prototype of Building A, a force increase for displacement larger than 50mm is observed which reduces the efficiency. For smaller amplitudes the efficiency would be larger in the case of Building A.

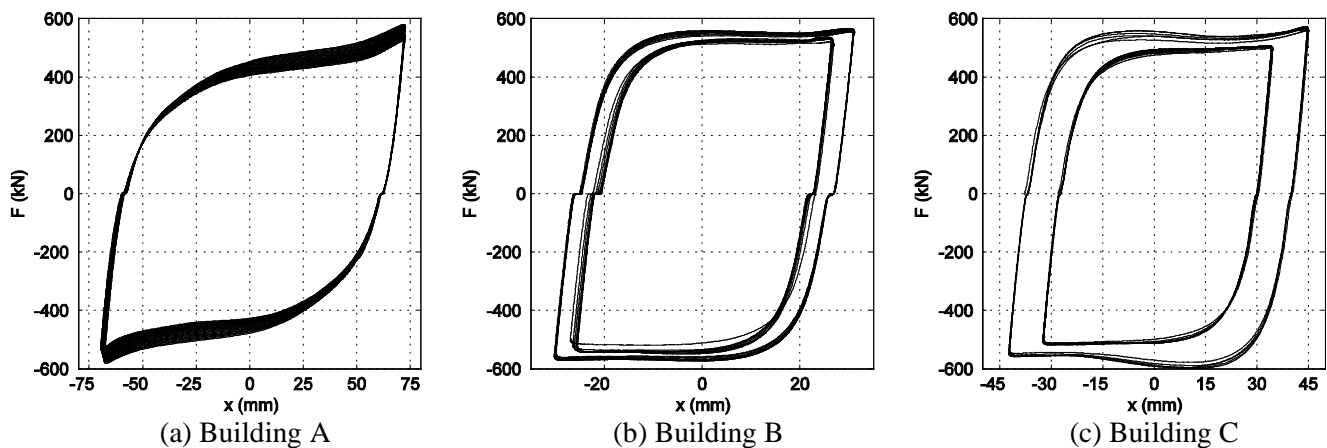


Figure 9 - Force displacement constitutive relationship of prototype tests.

## 6. Implementation of TADAS dampers

After successful prototype testing for each of the three building cases presented, the TADAS devices were manufactured and installed in the structures built between 2013 and 2015. Shown in Figure 10 are some pictures with the installed TADAS devices in the coupling beams. The TADAS devices were bolted to the coupling beams, and hence, the device could be easily replaced in case it would be necessary. However, this situation is unlikely since the devices have a high energy dissipation capacity as already shown. In Figure 1, a schematic view of the installation of the TADAS device in a coupling beam is shown. Shear forces are transferred from the TADAS to the concrete by studs, and tension forces and bending moments by couplers to the reinforcing bars. In the case of a fixed connection Type II presented in Figure 1, stop plates are used to eliminate shear slip between the base plate of the TADAS device and the anchorage plate since a slip-free friction connection was not possible. Nevertheless, after the curing of concrete, the bolts should be tightened to eliminate axial slip in the bolts, thus resulting in a stiff connection of the TADAS device to the coupling beam.

Compared to other energy dissipation solutions, one advantage of the TADAS devices installed in coupling beams is the stiffness and damping provided by the devices without the need of metallic braces. Therefore, the installation is very simple, fast, and can be executed by any construction company. In Figure 10 it can be observed that for Building A, the coupling beams were detached from the slab, while for Buildings B and C they are at the slab level. Therefore, in these cases the beam must be separated from the slab by an expansion joint to allow for the motion. Otherwise the relative displacement between the ends of the coupling beams would induce plastic deformation and damage of the slab during the earthquake, which needs to be avoided. This detail has to be considered by architects and other specialists during the design phase of the building.

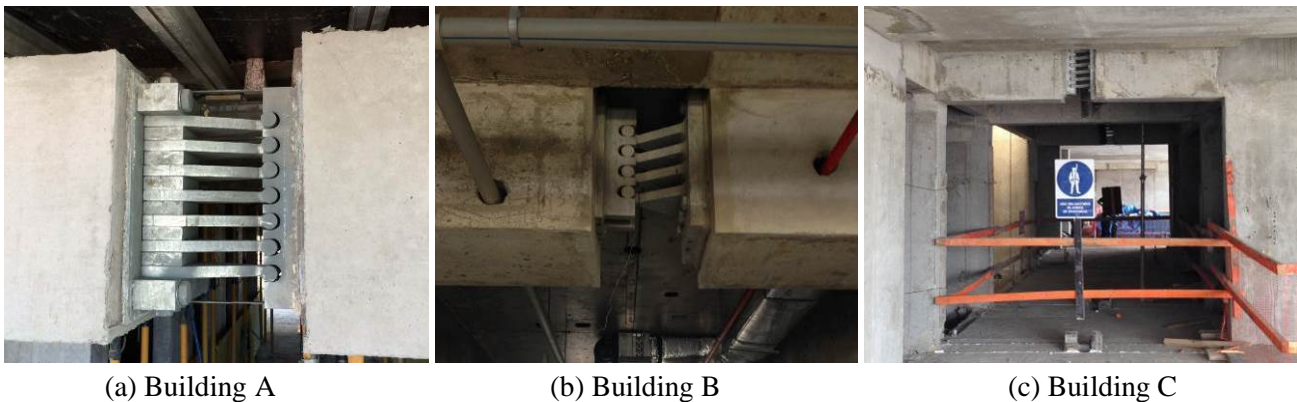


Figure 10 - TADAS devices installed in the three different buildings.

## 7. Conclusion

TADAS devices were successfully designed, tested, and installed in coupling beams of shear walls in three different recently built RC buildings. Placing TADAS devices in coupling beams is an interesting solution for owners, architects and constructors because cost and architectural impact is low, while effectiveness in response reduction is considerable. In this case, the design goal is to concentrate plastic deformation in the triangular metallic plates while keeping the supporting RC concrete beams within the elastic range.

Building design using metallic dampers can be easily accomplished using available commercially software. However, it is of the utmost importance for designers to know the limitations of each software to obtain representative results of the analysis that can truly estimate the earthquake demand on the dampers and the actual building performance. Simulations in this case show that the RMS inter-story drifts are reduced in average for the three buildings in 21.8%. Similar reductions are obtained for other response quantities such as roof displacement, absolute roof acceleration, and base shear.

In these cases, the TADAS devices were designed using a simple model to predict the force displacement constitutive relationship, stiffness, and fatigue life of the triangular plates. To obtain good model predictions, the



stress-strain constitutive relationship and the fatigue life cycle of the mild steel used was experimentally determined considering as-built manufacturing conditions as welding and heat treatment. A good design is always a trade-off between high stiffness for the TADAS damper and a high resistance to fatigue.

Using single plates and full scale prototypes, the designed TADAS devices were validated prior to installation. Thereby, it is observed that the force-displacement constitutive relationship is very stable and results in a very ductile energy dissipation device. Testing confirmed that force-displacement constitutive relationship of the TADAS dampers was nearly rate-independent, or essentially independent of test velocity within the applied range of frequencies. Furthermore, it is important to evaluate the fatigue life for the device, so the dissipated energy of the tested device at constant amplitudes can be compared with the dissipated energy obtained in earthquake simulations. For any of the building implementations, the designed devices accept at least three maximum considered earthquakes. Moreover, the connection proposed for the TADAS device to the coupling beam is appropriate as proven by the prototype tests.

Manufacturing of TADAS devices is simple and the installation of the devices in this solution is fast and straight forward with minimum impact on the construction process of the building. Hence, this experience shows that TADAS devices installed in beams that coupled shear walls can be an effective inexpensive alternative relative to other more sophisticated uses of the same dampers as well as other energy dissipation solutions.

## 8. Acknowledgement

The authors would like to thank the structural engineers Marcos Tinman and Alejandro Muñoz from Prisma Ingenieros and the personnel of the Seismic Isolation and Energy Dissipation Laboratory at DICTUC of the Pontificia Universidad Católica de Chile. The research of one of the authors of this paper has been sponsored by FONDECYT through Grant 1141187 and by the National Research Center for Integrated Natural Disaster Management CONICYT/FONDAP/15110017.

## 9. References

- [1] Tsai KC, Chen HW, Hong CP, Su YF (1993): Design of steel triangular plate energy absorbers for seismic-resistant construction, *Earthquake Spectra*, **9** (3), 505-528.
- [2] Whittaker A, Bertero V, Alonso J, Thompson C (1989): Earthquake simulator testing of steel plate added damping and stiffness elements, Report No. UCB/EERC-89/02, Earthquake Engineering Research Center, University of California, Berkeley, USA.
- [3] Briones B, De La Llera JC (2014): Analysis, design and testing of an hourglass-shaped copper energy dissipation device. *Engineering Structures*, **79**, 309-321.
- [4] Li R, Zhang Y, Tong LW (2014): Numerical study of the cyclic load behavior of AISI 316L stainless steel shear links for seismic fuse device. *Frontiers of Structural and Civil Engineering*, **8** (4), 414-426.
- [5] Vasdravellis G, Karavasilis TL, Uy B (2014): Design rules, experimental evaluation and fracture models for high-strength and stainless-steel hourglass shape energy dissipation devices. *Journal of Structural Engineering (ASCE)*, **140** (11).
- [6] Mahmoudi M, Abdi MG (2012): Evaluating response modification factors of TADAS frames. *Journal of Constructional Steel Research*, **71**, 162-170.
- [7] Shamshiri Dareini H, Hosseini Hashemi B (2011): Use of dual system in TADAS dampers to improve seismic behavior of buildings in different levels. *Procedia Engineering*, **14**, 2788-2795.
- [8] Hassanieh AH, Zarfam P, Mofid M (2012): Assessment of seismic behavior of 3D asymmetric steel buildings retrofitted with TADAS device based on incremental dynamic analysis (IDA). *15<sup>th</sup> World Conference on Earthquake Engineering*, Lisbon, Portugal.
- [9] Alehashem SMS, Keyhani A, Pourmohammad H (2008): Behavior and performance of structures equipped with ADAS & TADAS dampers (a comparison with conventional structures). *14<sup>th</sup> World Conference on Earthquake Engineering*, Beijing, China.



- [10] Massone L, Bonelli P, Lagos R, Lüders C, Moehle J, Wallace J (2012): Seismic design and construction practices for RC structural wall buildings. *Earthquake Spectra*, **28** (S1), S245–S256.
- [11] Moroni O (2011): Concrete shear wall construction, World Housing Encyclopedia, <http://www.world-housing.net/>, 6pp.
- [12] Wang T, Guo X, He X, Du Y, Duan C (2012): Seismic behavior of high-rise concrete shear-wall buildings with hybrid coupling beams. *15<sup>th</sup> World Conference on Earthquake Engineering*, Lisbon, Portugal.
- [13] Choi KS, Kim HJ (2014): Strength demand of hysteretic energy dissipating devices alternative to coupling beams in high rise building. *International Journal of High-Rise Buildings*, **3** (2), 107-120.
- [14] Pan C, Weng DG (2011): Study on seismic performance of coupled shear walls with vertical dampers. *Advanced Materials Research*, **163-167**, 4185-4193.
- [15] Mao CX, Wang ZY, Zhang LQ, Li H, Ou JP (2012): Seismic performance of RC frame-shear wall structure with novel shape memory alloy dampers in coupling beams. *15<sup>th</sup> World Conference on Earthquake Engineering*, Lisbon, Portugal.
- [16] Kim HJ, Choi KS, Oh SH, Kang CH (2012): Comparative study on seismic performance of conventional RC coupling beams and hybrid energy dissipative coupling beams used for RC shear walls. *15<sup>th</sup> World Conference on Earthquake Engineering*, Lisbon, Portugal.
- [17] Chang KL, Rees SJW, Carroll C, Clandening K (1999): The use of Triangular Added Damping and Stiffness (TADAS) devices in the design of the Core Pacific City Shopping Center. *Proceedings of the Second International Conference on Advances in Steel Structures*, Hong Kong, China.
- [18] Chang KC, Hwang JS, Lee SN (2004): Status of application of passive control technologies in Taiwan. *13<sup>th</sup> World Conference on Earthquake Engineering*, Vancouver, Canada.
- [19] Perry CL, Fierro EA, Sedarat H, Scholl RE (1993): Seismic upgrade in San Francisco using energy dissipation devices. *Earthquake Spectra*, **9** (3), 559-579.
- [20] Martinez Romero E (1993): Experiences on the use of supplementary energy dissipators on building structures. *Earthquake Spectra*, **9** (3), 581-625.
- [21] Li G, Li H (2008): Earthquake-resistant design of RC frame with “dual functions” metallic dampers. *14<sup>th</sup> World Conference on Earthquake Engineering*, Beijing, China.
- [22] Computers & Structures, Inc. ETABS v.9.7.4. 2011. Berkeley, California, USA.
- [23] Wen YK (1976): Method of random vibration of hysteretic systems. *Journal of Engineering Mechanics (ASCE)*, **102** (2), 249-263.
- [24] Official Chilean Standard (2013): NCh2745.Of.2013, Analysis and design of buildings with base isolation (in Spanish), Instituto Nacional de Normalización, INN.